International Journal of Minerals, Metallurgy and Materials
Volume 24, Number 12, December 2017, Page 1379
DOI: 10.1007/s12613-017-1530-2

Effect of hot-dip galvanizing processes on the microstructure and mechanical properties of 600-MPa hot-dip galvanized dual-phase steel

Chun-fu Kuang[1)], *Zhi-wang Zheng*[1)], *Min-li Wang*[1)], *Quan Xu*[1)], *and Shen-gen Zhang*[2)]

1) State Key Laboratory of Vanadium and Titanium Resources Comprehensive Utilization, Research Institute of Pangang Group, Panzhihua 617000, China
2) Institute for Advanced Materials and Technology, University of Science and Technology Beijing, Beijing 100083, China
(Received: 31 January 2017; revised: 1 August 2017; accepted: 3 August 2017)

Abstract: A C–Mn dual-phase steel was soaked at 800°C for 90 s and then either rapidly cooled to 450°C and held for 30 s (process A) or rapidly cooled to 350°C and then reheated to 450°C (process B) to simulate the hot-dip galvanizing process. The influence of the hot-dip galvanizing process on the microstructure and mechanical properties of 600-MPa hot-dip galvanized dual-phase steel (DP600) was investigated using optical microscopy, scanning electron microscopy (SEM), transmission electron microscopy (TEM), and tensile tests. The results showed that, in the case of process A, the microstructure of DP600 was composed of ferrite, martensite, and a small amount of bainite. The granular bainite was formed in the hot-dip galvanizing stage, and martensite islands were formed in the final cooling stage after hot-dip galvanizing. By contrast, in the case of process B, the microstructure of the DP600 was composed of ferrite, martensite, bainite, and cementite. In addition, compared with the yield strength (YS) of the DP600 annealed by process A, that for the DP600 annealed by process B increased by approximately 50 MPa because of the tempering of the martensite formed during rapid cooling. The work-hardening coefficient (n value) of the DP600 steel annealed by process B clearly decreased because the increase of the YS affected the computation result for the n value. However, the ultimate tensile strength (UTS) and elongation (A_{80}) of the DP600 annealed by process B exhibited less variation compared with those of the DP600 annealed by process A. Therefore, DP600 with excellent comprehensive mechanical properties (YS = 362 MPa, UTS = 638 MPa, A_{80} = 24.3%, n = 0.17) was obtained via process A.

Keywords: hot-dip galvanizing process; dual-phase steel; microstructure; mechanical properties

1. Introduction

Researchers have recently been demonstrating growing interest in advanced high-strength steels for bumper beams and B pillars, such as dual-phase (DP) steel, transformation-induced-plasticity (TRIP) steel, complex phase steel, and quenching and partitioning (Q&P) steel, because of their optimal combination of low yield strength (YS), high ultimate tensile strength (UTS), continuous yielding, and good ductility [1–4]. The microstructure of DP steel is composed of a soft ferrite matrix and hard martensite islands; the ferrite phase provides good plasticity, whereas the martensite phase controls the strength [5–6].

In the hot-dip galvanizing annealing stage, strip steel is maintained at 450–460°C for 10–40 s for galvanization. Therefore, the transformation of supercooled austenite into bainite during galvanization leads to less martensite phase in DP steel after final cooling. Consequently, the YS increases and the UTS decreases [7–8]. In hot-dip galvanized DP steel, the volume fraction of martensite plays an important role in governing the mechanical properties, including YS, UTS, and elongation (A_{80}), among other properties. Consequently, to obtain a high martensite volume fraction and comprehensive mechanical properties, Sayed and Kheirandish [9] and Li *et al.* [10] adjusted the chemical composition or the annealing process of DP steel.

In the present work, the effect of the hot-dip galvanizing process on the microstructure and mechanical properties of DP600 was investigated. The aim of the current work is to provide a fundamental understanding of the microstructure evolution of DP600 during the rapid cooling and hot-dip galvanizing stages and to elucidate the relationship among

Corresponding author: Chun-fu Kuang E-mail: kuangchunfu@126.com

the hot-dip galvanizing process, the volume fraction of martensite, and the mechanical properties of DP600.

2. Experimental

Cold-rolled C–Mn steel with a chemical composition of 0.05wt%–0.10wt% C, 0.10wt%–0.60wt% Si, 1.20wt%–1.80wt% Mn, 0.010wt% P, 0.005wt% S, 0.05wt%–0.25wt% Mo, 0.10wt%–0.30wt% Cr, and 0.02wt%–0.06wt% Al was used in this research. After being reheated to 1230°C for 2 h and hot-rolled to 3.5 mm, the steels were coiled at 650°C and then cold-rolled to 1.2 mm in thickness. Fig. 1 shows a schematic of the hot-dip galvanizing annealing process. The steels were heated to 800°C for 90 s, then either rapidly cooled to 450°C and held for 30 s (process A) or rapidly cooled to 350°C and then reheated to 450°C (process B) to simulate the hot-dip galvanizing process. In both processes, the samples were finally cooled to room temperature in air.

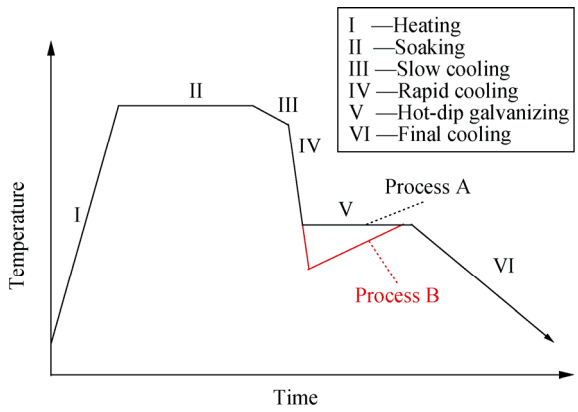

Fig. 1. Schematic of the hot-dip galvanizing annealing process.

Optical and SEM microscopic observations were carried out after the samples were etched in 4vol% nital solution. Tensile samples with a gauge length of 80 mm were cut from the as-annealed sheets according to ISO standard 10113. Tensile tests were carried out on an Instron tensile machine at a constant cross-head speed of 3 mm·min^{-1}. At least three samples were tested for each condition, and the average value was calculated.

3. Results and discussion

3.1. Microstructure

In the cold-rolled steel, recovery, recrystallization, and austenite transformation occur sequentially during heating [11]. The DP600 with a microstructure composed of ferrite, martensite, and bainite was obtained after the austenite was transformed into martensite by final cooling. The microstructures of the DP600 steel samples developed by two different hot-dip galvanization processes are shown in Fig. 2. The microstructure of DP600 mainly consisted of martensite islands and a small amount of bainite dispersed in the ferrite matrix (Fig. 2(a)). Meanwhile, the tempering of martensite did not occur when the DP600 was hot-dip galvanizing annealed via process A. Thus, carbides are not observed in the pure martensite islands.

The microstructures of the DP600 samples annealed by processes A and B differ. As shown in Fig. 2(b), numerous non-martensite and carbide particles appeared in the ferrite matrix. This phenomenon is attributed to the transformation of supercooled austenite into bainite and to the decomposition of martensite into ferrite and carbide. This result is in agreement with that reported by Ye *et al.* [12]. During the stage of rapid cooling to 350°C, the supercooled austenite transformed into martensite because the cooling temperature was below the martensite transformation start temperature (M_s). The intermediate martensite formed during rapid cooling decomposed into ferrite and cementite during the reheating and hot-dip galvanizing stage because the martensite was tempered at a hot-dip galvanization temperature of 450°C [13]. As evident in Fig. 2(b), a large amount of

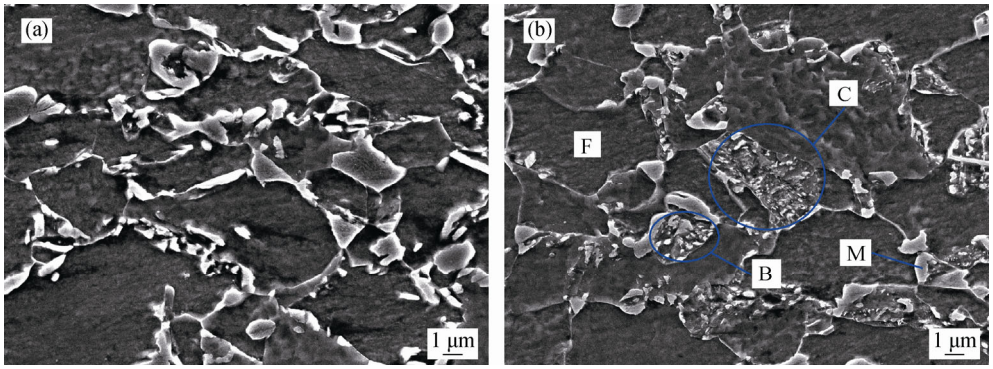

Fig. 2. SEM micrographs of the hot-dip galvanized DP600 samples annealed by process A (a) and process B (b) (F: ferrite; M: martensite; B: bainite; C: cementite).

cementite is observed due to the decomposition of martensite. The decomposed martensite is metastable and large because of its low average contents of carbon and microalloying elements. Furthermore, the amount of mobile dislocations located in the grain interior decreased because of the tempering. Meanwhile, the supercooled austenite transformed into bainite because the hot-dip galvanization temperature of 450°C fell within the bainite transformation zone [14]. By contrast, the residual supercooled austenite transformed into a martensite phase during the final cooling stage. As a result, the microstructure of DP600 annealed by process B was composed of ferrite, martensite, bainite, and cementite.

3.2. Mechanical properties

Table 1 shows the mechanical properties of DP600 developed by the two different hot-dip galvanization processes. Both the hot-dip galvanized DP600 steel annealed by process A and process B satisfy the standard of mechanical properties for DP600. Compared with the YS and yield ratio of the hot-dip galvanized DP600 steel for process A, those of the steel for process B were obviously enhanced; in addition, the UTS and elongation showed less variation and the work-hardening coefficient (n value) and product of the strength and elongation (UTS × A_{80}) decreased substantially in the case of the DP600 annealed by process B.

Table 1. Mechanical properties of hot-dip galvanized DP steels

Process	YS / MPa	UTS / MPa	A_{80} / %	n	Yield ratio	UTS × A_{80}
A	362	638	24.3	0.17	0.57	15500
B	411	629	23.5	0.13	0.65	14780
Standard	340–420	≥600	≥20.0	≥0.14	—	—

In DP600, the YS mainly depends on the ferrite phase, including the ferrite grain size, mobile dislocation density, and carbide precipitates. The UTS and elongation mainly depend on the martensite phase. Generally, the UTS increases and the elongation decreases with increasing martensite volume fraction [15]. Tempering of martensite did not occur when DP600 was annealed by process A. Thus, its microstructure was composed of ferrite, martensite, and a small amount of bainite. In the martensite transformation stage, free dislocations were produced through volume expansion that occurred during the transformation of austenite to martensite [16]. Fig. 3 shows a TEM micrograph of DP600 developed by process A. The microstructure was composed of ferrite and martensite, and numerous dislocations occurred at the ferrite–martensite interface. In the plastic deformation stage, the mobile dislocations can slip under the condition of low external stress [17]. Consequently, a low YS, low yield ratio, and high n value occurred in the case of DP600 annealed using process A.

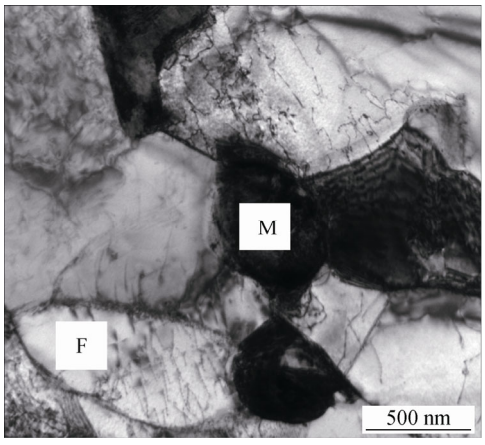

Fig. 3. TEM micrograph of DP600 annealed by process A.

In process B, the intermediate martensite first formed during rapid cooling to 350°C and was then tempered at the hot-dip galvanization temperature of 450°C. Therefore, the martensite decomposed into ferrite and cementite during the reheating and hot-dip galvanization stage (Fig. 2(b)). The precipitation of carbide led to the strong pinning of free dislocations during plastic deformation. In the tempering stage, the supersaturated solute C atoms in the martensite phase would dissolve and segregate to mobile dislocations located at the ferrite–martensite interface, leading to strong pinning due to the formation of a Cottrell atmosphere or carbides [18]. In addition, the decrease in the volume fraction of martensite formed in the final cooling after the hot-dip galvanization process led to fewer free dislocations in the ferrite interior. Meanwhile, the mobile dislocations disappeared during tempering, leading to a decrease in the number of free dislocations. Consequently, the YS of DP600 annealed by process B increased. However, the microstructure of DP600 annealed by process B was composed of ferrite, martensite, bainite, and cementite. Although the martensite was decomposed during the reheating and hot-dip galvanization stage, the volume fraction of martensite decreased marginally because only the metastable and large-sized martensite was tempered. Therefore, the UTS decreased slightly.

In the plastic deformation stage, the n value depends on the stress and strain and can be calculated using Eq. (1) [19]:

$$\sigma = K \cdot \varepsilon^n \quad (1)$$

where σ is the stress, ε is the strain, K is the proportionality coefficient, and n is the work-hardening coefficient. Assuming that the initial and maximum stresses are σ_1 and σ_2 and that the initial and maximum strains are ε_1 and ε_2, respectively, the n value can be calculated as

$$n = \ln\frac{\sigma_1}{\sigma_2} \Big/ \ln\frac{\varepsilon_1}{\varepsilon_2} \quad (2)$$

According to Table 1, compared with the UTS and elongation of the hot-dip galvanized DP600 steel annealed using process A, those of the hot-dip galvanized DP600 annealed using process B exhibit less variation. Thus, in this work, YS plays an important role in determining the n value of the hot-dip galvanized DP600. According to Eq. (2), with an increase in the initial stress, the work-hardening coefficient of DP600 obviously decreases. In the samples subjected to hot-dip galvanizing process B, numerous carbides precipitated and the density of free dislocations decreased because of the martensite tempering [20]. Consequently, as the YS increases, the n value decreases.

Furthermore, in the reheating and hot-dip galvanizing stage, the hardness of the martensite would decrease because of the tempering behavior. Consequently, the pileup of dislocations because of the slip of mobile dislocations to the ferrite–martensite interface would be substantially diminished. Therefore, as the interaction between the free dislocations and martensite is reduced, the work-hardening coefficient decreases [21]. In summary, as a result of annealing process B, the YS and yield ratio increase and the n value decreases.

4. Conclusions

(1) In the DP600 annealed by process A, the microstructure was composed of ferrite, martensite, and a small amount of bainite. By contrast, the microstructure of DP600 annealed by process B was composed of ferrite, martensite, bainite, and cementite because of the transformation of supercooled austenite into bainite and the decomposition of martensite into ferrite and carbide.

(2) Compared with the YS and yield ratio of the DP600 annealed using process A, those of the DP600 annealed using process B were enhanced; in addition, the UTS and elongation showed less variation and the n value and product of strength and elongation decreased in the case of the sample subjected to process B. DP600 with excellent comprehensive mechanical properties (YS = 362 MPa, UTS = 638 MPa, A_{80} = 24.3%, n = 0.17) was obtained in the case of process A.

Acknowledgements

This work was financially supported by the National Natural Science Foundation of China (Nos. U1360202, 51472030, and 51502014).

References

[1] Y.L. Kang, *Theory and Technology of Processing and Forming for Advanced Automobile Steel Sheets*, Metallurgical Industry Press, Beijing, 2009, p. 230.

[2] P. Li, J. Li, Q.G. Meng, W.B. Hu, and C.F. Kuang, Influence of rapid heating process on the microstructure and tensile properties of high-strength ferrite–martensite dual-phase steel, *Int. J. Miner. Metall. Mater.*, 22(2015), No. 9, p. 933.

[3] H.T. Jiang, B.T. Zhuang, X.G. Duan, Y.X. Wu, and Z.X. Cai, Element distribution and diffusion behavior in Q&P steel during partitioning, *Int. J. Miner. Metall. Mater.*, 20(2013), No. 11, p. 1050.

[4] H.T. Jiang, W. Ding, D. Tang, and W. Huang, Mechanical property and microstructural characterization of C-Mn-Al-Si hot dip galvanizing TRIP steel, *J. Iron Steel Res. Int.*, 19(2012), No. 8, p. 29.

[5] C.F. Kuang, S.G. Zhang, J. Li, J. Wang, and H.F. Liu, Effect of pre-strain and baking parameters on the microstructure and bake-hardening behavior of dual-Phase steel, *Int. J. Miner. Metall. Mater.*, 21(2014), No. 8, p. 766.

[6] A.G. Kalashami, A. Kermanpur, E. Ghassemali, A. Najafizadeh, and Y. Mazaheri, The effect of Nb on texture evolutions of the ultrafine-grained dual-phase steels fabricated by cold rolling and intercritical annealing, *J. Alloys Compd.*, 694(2017), No. 2, p. 1026.

[7] I. Aslam, B. Li, R.L. Martens, J.R. Goodwin, H.J. Rhee, and F. Goodwin, Transmission electron microscopy characterization of the interfacial structure of a galvanized dual-phase steel, *Mater. Charact.*, 120(2016), No. 10, p. 63.

[8] E.B. Pan, H.S. Di, G.W. Jiang, and C.R. Bao, Effect of heat treatment on microstructures and mechanical properties of hot-dip galvanized DP steels, *Acta Metall. Sin.*, 27(2014), No. 3, p. 469.

[9] A.A. Sayed and S. Kheirandish, Affect of the tempering temperature on the microstructure and mechanical properties of dual phase steels, *Mater. Sci. Eng. A*, 532(2012), p. 21.

[10] C.S. Li, Z.X. Li, Y.M. Cen, B. Ma, and G. Huo, Microstructure and mechanical properties of dual phase strip steel in the overaging process of continuous annealing, *Mater. Sci. Eng. A*, 627(2015), p. 281.

[11] C.F. Kuang, S.G. Zhang, J. Li, J. Wang, and D.C. Xu, Effect of rapid heat treatment on bake hardening behavior of a low carbon steel, *J. Mater. Res.*, 28(2014), No. 4, p. 263.

[12] J.Y. Ye, Z.Z. Zhao, Z.G. Wang, and A.M. Zhao, Microstructure and mechanical properties of 1000 MPa grade C-Si-Mn-Nb cold-rolled dual-phase steel, *Trans. Mater. Heat Treat.*, 34(2013), No. 4, p. 138.

[13] A. Kamp, S. Celotto, and D.N. Hanlon, Effects of tempering on the mechanical properties of high strength dual-phase steels, *Mater. Sci. Eng. A*, 538(2012), p. 35.

[14] E. Abbasi and W.M. Rainforth, Microstructural evolution during bainite transformation in a vanadium microalloyed TRIP-assisted steel, *Mater. Sci. Eng. A*, 651(2016), p. 822.

[15] M. Calcagnotto, D. Ponge, and D. Raabe, Microstructure control during fabrication of ultrafine grained dual-phase steel: characterization and effect of intercritical annealing parameters, *ISIJ Int.*, 52(2012), No. 5, p. 874.

[16] C.F. Kuang, Z.W. Zheng, G.T. Zhang, J. Chang, S.G. Zhang, and B. Liu, Effects of overaging temperature on the microstructure and properties of 600 MPa cold-rolled dual–phase steel, *Int. J. Miner. Metall. Mater.*, 23(2016), No. 8, p. 943.

[17] S.P. Tsai, C.H. Jen, H.W. Yen, C.Y. Chen, M.C. Tsai, C.Y. Huang, Y.T. Wang, and J.R. Yang, Effects of interphase TiC precipitates on tensile properties and dislocation structures in a dual phase steel, *Mater. Charact.*, 123(2017), No. 2, p. 153.

[18] X. Fang, Z. Fan, B. Ralph, P. Evans, and R. Underhill, Effects of tempering temperature on tensile and hole expansion properties of a C–Mn steel, *J. Mater. Process. Technol*., 132 (2003), No. 1-3, p. 215.

[19] Y. Mazaheri, A. Kermanpur, A. Najafizadeh, and N. Saeidi, Effects of initial microstructure and thermomechanical processing parameters on microstructures and mechanical properties of ultrafine grained dual phase steels, *Mater. Sci. Eng. A*, 612(2014), p. 54.

[20] S. Gündüz, Effect of chemical composition, martensite volume fraction and tempering on tensile behaviour of dual phase steels, *Mater. Lett.*, 63(2009), No. 27, p. 2381.

[21] A.G. Kalashami, A. Kermanpur, E. Ghassemali, A. Najafizadeh, and Y. Mazaheri, Correlation of microstructure and strain hardening behavior in the ultrafine-grained Nb-bearing dual phase steels, *Mater. Sci. Eng. A*, 678(2016), p. 215.